The World of Surface Coatings Is Centered Around the Glass Transition Temperature, *But Which One?* Part I

by **Greg Curtzwiler**, **Mark Early**, **Diana Gottschalk**, **Christina Konecki**, **Robert Peterson**, **Steven Wand**, and **James W. Rawlins**

School of Polymers and High Performance Materials,

The University of Southern Mississippi

Polymeric materials are employed in a wide variety of applications, and whether the desired performance is a mechanical response, specific permeability, chemical reactivity, or general response to any given stimuli, the target properties are strongly affected by the molecular dynamics of all blended materials and reactants. The molecular dynamics of amorphous materials are controlled by the resulting glass transition temperature (T_g). This two-part article reviews the importance of T_g in polymeric coatings, and emphasizes the shifting nature of a material's T_g throughout the service lifetime. In attempting to simplify a complex combination of material dynamics, a polymer's T_g has often been utilized as a single value parameter throughout history. While correlations exist between the T_g and many important material properties, a single T_g value does not communicate the multifaceted material dynamics involved in formulation, application, film formation, cure, or *in-service* use.

INTRODUCTION

Each coating's glass transition temperature (T_g) is a net result of the effects of its constituents and the compositions and ratios of its polymeric building blocks. In many cases, T_gs correlate with performance parameters. In this article, we limit our discussion to amorphous polymers and matrix materials used to form surface coatings (intentionally excluding semicrystalline and crystalline polymers, as these relationships become even more complex). The T_g is a very intricate concept and is not adequately represented by a single value, even though it is an excellent starting point for understanding surface coating dynamics. A number of methods are available to measure T_g that typically provide a range of values with subtle to significant differences. Furthermore, the T_g range, e.g., the difference between dry and wet T_g for the same coating, clouds our understanding of the T_g values' correlation with material properties. It is imperative to understand when, how, and why coatings perform as they do from varying application methods, differing cure profiles, and a wide array of environmental conditions. Surprisingly, the general literature considers T_g to be a single number without considering the importance of the T_g range and differences that vary with changes in formulation, application, cure and crosslinking, and environmental parameters. In this article, the term *in-service* T_g is defined as the T_g measured under the specific conditions at that moment in time.

Figure 1 simplistically presents the range of T_gs from one prepolymer, a single crosslinker, and a blend of two solvents in combination with three levels of water during the service life. The graphs show the dramatic differences between the low and high T_g values. The bottom right graph reveals that the combined effect of residual solvent and ambient moisture results in an in-service T_g ranging from 55 to 107 °C with identical raw material mass balances. The T_g differences are even more dramatic when faster-evaporating solvents and ambient cure profiles are used in combination, whereby the cure and solvent evaporation result in vitrification limiting chemical conversion and potentially trapping higher concentrations of solvents.

Presented as the Plenary Lecture at the Waterborne, High-Solids and Powder Coatings Symposium, February 24-28, 2014 in New Orleans, LA.

WHAT MATERIALS EXHIBIT A T_g?

A variety of materials and T_g ranges are shown in *Table* 1. In general, glassy materials are generated by cooling a wide variety of materials at sufficiently high rates to solidify or freeze them into an amorphous glassy state, often cooled from the melt state. Either the cooling rate or the materials' organizational structure (often both rate and structure) limit the combined materials' ability to crystallize, yet solidification occurs.[1] When focused on coatings, we also need to consider the polymer's interactions with pigments, additives, plasticizers, residual solvents, the substrate, and the influence of environmental conditions.

The scientific literature is replete with examples where scientists have combined evaporation rates, solvent retention, hydroplasticization, and other environmental factors to estimate, quantify, and understand the momentary and/or practical in-service T_g between selection and use. The practical in-service T_g prediction and rate of T_g change and viscosity is invaluable for prediction of material state, rate of state change, and ultimate physical states for morphology, film formation, and polymer/surface coating performance. For example, 10% trapped residual solvent results in less hardness, higher impact resistance, and better flexibility, but only on a temporary basis. Early laboratory results are often misleading and performance under extended service considerations are required to understand material properties as a function of time.

Table 1—T_g Ranges for a Variety of Classes

Material	T_g Range (°C)	Specific Example
Polymers[2]	-173 – ~ 500	Poly(2-hydroxyethyl acrylate) (syndiotactic) (377 °C)
Plasticizers (Coalescing aids)[3]	-127 – -67	Propylene glycol methyl ether (-125 °C)
Water[4]	-136	
Solvents[5-9]	-196 – -84	
Ionic solvents[10]	159 – 409	1-alkyl imidazolium (174 – 211 °C)
Proteins[11-17]	146 – 256	Lysozyme (179 °C)
Amino acids[12]	232 – 931	Methionine (362 °C)
Sugars[18-21]	65 – 286	Sucrose (76 °C)
Silicate glasses[22-26]	423 – 1100	Pyrex (565 °C)
Phosphate glasses[26-32]	542 – 763	$Li_3Fe_2P_3O_{12}$ (724 °C)
Fluoride glasses[33-36]	262 – 332	53% ZrF_4, 20% BaF_2, 4% LaF_3, 3% AlF_3, 20% NaF (262 °C)
Amorphous metals[37,38]	151 – 403	$Mg_{80}Ni_{10}Nd_{10}$ (181 °C)

WHAT IS A T_g?

In simple terms, the T_g is the temperature at which amorphous, noncrystalline, polymer morphological domains shift between glassy and rubbery

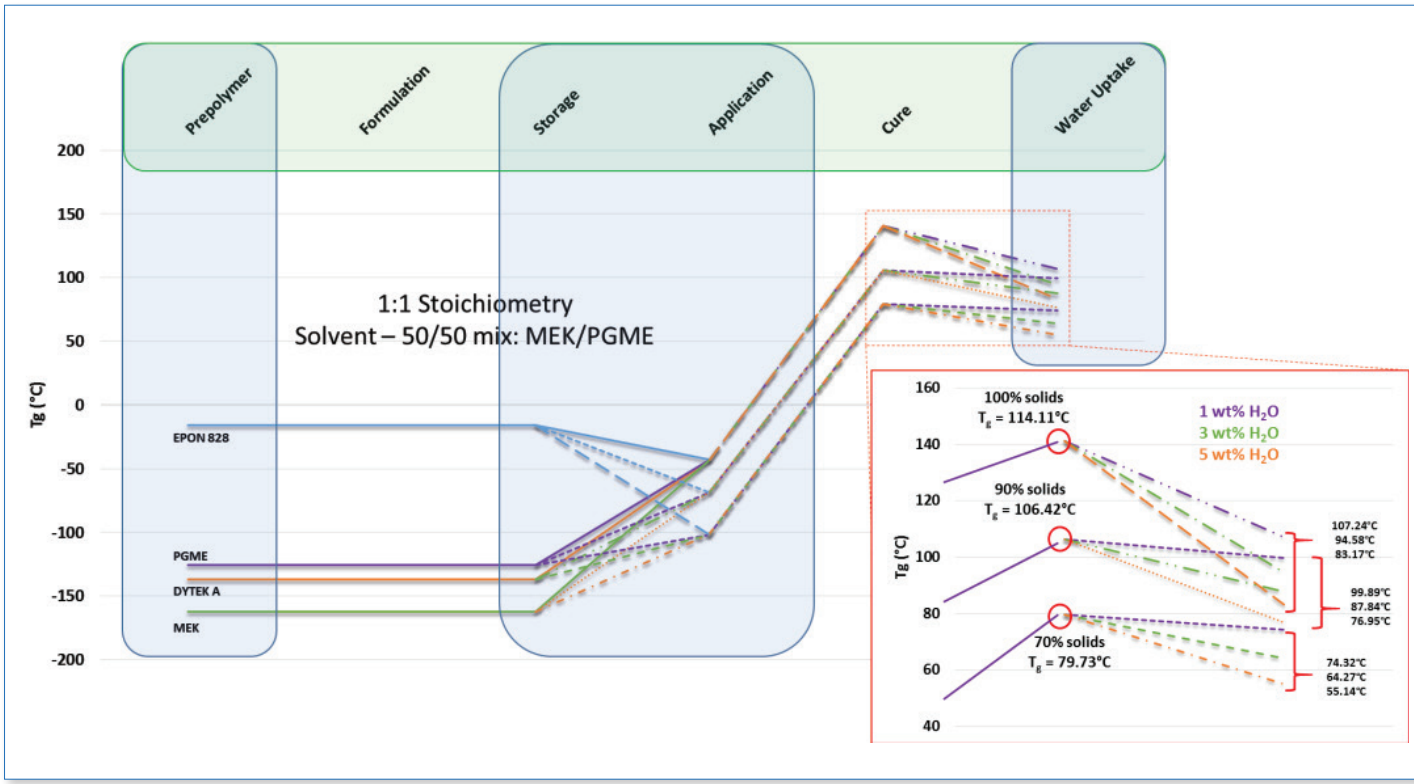

Figure 1—Overview of the life of a surface coating relative to the material's T_g during each period: raw materials, formulation and storage, application, cure, and utilization.

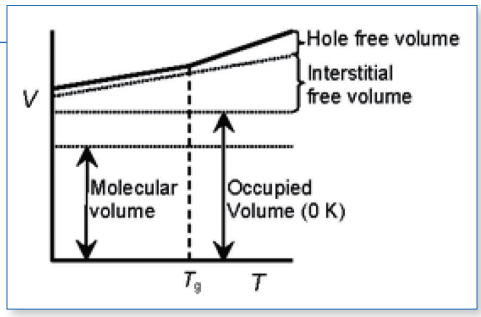

Figure 2—Specific volume representation of volume components.[46]

physical states. Polymers are classified into physical states based upon the relative difference between the T_g and the application/use temperature (T); these states are glassy ($T < T_g$), leathery ($T \approx T_g$), or rubbery ($T > T_g$).[39] Macroscopically, the physical changes that occur at the T_g are similar for all materials. Upon heating beyond the T_g, initiation of flow occurs, along with increased tack and loss of modulus or softening.[39,40] It is observed in crosslinked materials that the sharp loss in modulus is followed by a gradual increase as the temperature continues to rise beyond T_g.[41] Atomic and bond nature, number, size, and density each result in differences in material responses to thermal and mechanical forces based upon the summation of intra- and inter-molecular forces.

Amorphous polymers most often respond to the addition of thermal energy by enabling increased amounts of rotational and translational motions. With sufficient thermal energy, the polymeric material begins to experience chain slipping, uncoiling, and varying degrees of conformational changes resulting in shifted entanglement partners.[42] Thermally, crossing of the T_g often implies overcoming the energy barrier of the combined secondary, tertiary, or quaternary affinities and

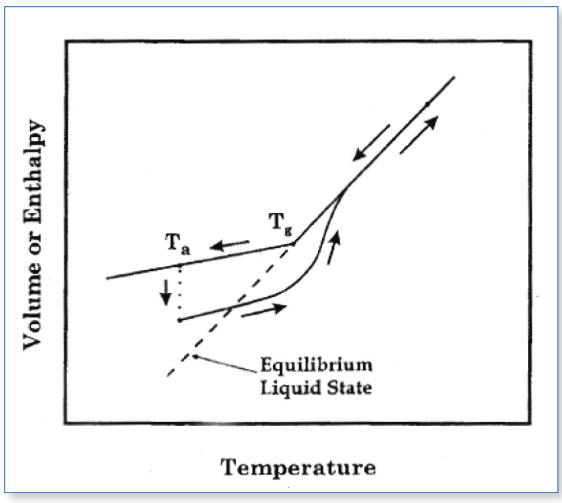

Figure 3—Cycle of aging: (1) cool below T_g, (2) densification, (3) reheat, and (4) enthalpic recovery. Illustration based on conclusions made by Scherer.[55]

bonds. Such chain-to-chain morphological changes occur without affecting the covalent bonds of polymer backbones.[43] A common T_g definition for polymers can thus be constructed as the onset of segmental motion.[44] Below the temperature where segmental motion is possible, smaller motions, e.g., side chain rotations, are observed that translate into differences for resistance to deformation, and yet, absence of bulk flow.

The chemical building blocks of a polymer, i.e., backbone, side chains, and chain-to-chain interactions, and how all the chemistry is connected plays a distinctively important role in determining which chain motions are possible at what temperature. Increased interchain interactions result in higher T_gs. There are several approaches to describing and understanding the T_g, and the directly relevant are described in brief below.

THE FREE VOLUME T_g THEORY

At the atomic level, a material's volume is the average sum of three components: (1) the space atoms physically take up, (2) interstitial volume between atoms associated with bonds or atomic packing, and finally, (3) voids or free volume (*Figure* 2). The atomic volume (van der Waals volume) is independent of temperature. The other occupied volume (the interstitial volume) component increases slightly with temperature due to larger oscillations between atoms. The free volume is nonlinearly affected by temperature. The void/free volume tends to be constant below the T_g, but increases with temperature above T_g.[45]

The free volume amount is nearly identical in each polymer at its respective T_g.[47] Most polymeric materials, regardless of composition, have similar thermal and mechanical characteristics at the T_g, e.g., almost all polymers have a viscosity of approximately 10^{21} Poise at T_g.[2] The free volume theory states that a consistent value of 2.5% free volume is required to achieve segmental motion. The T_g of a given polymer is determined to be the amount of energy required to expand the free volume beyond 2.5%. Differing environmental influences, e.g., metal or ceramic complex or affinity, result in higher levels of polymer organization, as is the case with substrates or pigment surfaces and the most closely associated polymeric materials. The T_g is not adequately explained purely on the basis of thermodynamic transitions. Differences in the heating/cooling rate shift the resulting values of T_g. The T_g is dependent on the rate of temperature change which is indicative of a kinetic component to the glass transition.[48]

THE KINETIC THEORY OF T_g

At a given temperature, each polymer possesses a specific equilibrium conformation and characteristic relaxation times for the side chains and backbone molecular motions.[49] These relaxations can be described conceptually using kinetic theory, where a given conformational change has a kinetic energy barrier to overcome. As a result, lower temperatures increase the time required for each constituent to move and relax. At higher temperatures, the relaxation times follow an Arrhenius behavior, but upon approaching the glassy state, this behavior often deviates and is better described using the Voge–Flucher–Tammann (VFT) equation.[50-52] In literature, a rearranged version derived by Williams, Landel, and Ferry in 1955, i.e., the WLF equation, is more commonly used.[53] Each polymer passes through a temperature upon cooling where these relaxation times become long enough that it acts as a solid material. By convention, this T_g is generally defined as the temperature where the primary relaxation time reaches 100 sec. The consequence of having such long relaxation times means that the polymer freezes into a nonequilibrium state, i.e., the glassy state.[54] When a polymer is cooled below its T_g at any cooling rate and then held isothermally for an extended period of time, sub-T_g relaxation occurs, resulting in a conformation closer to the equilibrium liquid (*Figure* 3).[48] This phenomenon is called aging, and can be understood using the kinetic theory of T_g. Aging is the result of allowing a polymer enough time to relax towards equilibrium.

HOW IS T_g MEASURED?

Numerous methods are used to measure T_g, a few of which are summarized in *Table* 2. The dominant methods employed in surface coatings are differential scanning calorimetry (DSC) and dynamic mechanical analysis (DMA), and are expanded upon for our discussion. It must be noted that the heating/cooling rates and frequency have noticeable influence on the measured glass transition temperature which can be attributed to the kinetic aspect of the glass transition phenomenon and the non-instantaneous heat transfer within the material. In general, faster heating rates will result in a higher apparent glass transition temperature than slower heating rates; increased frequencies have yielded similar results.[56] Additionally, there is a noticeable difference of the apparent T_g employing varying techniques [i.e., thermomechanical analysis (TMA) vs. DSC: *Figure* 4]. Such distinctions are important to note in order to accurately compare different systems.

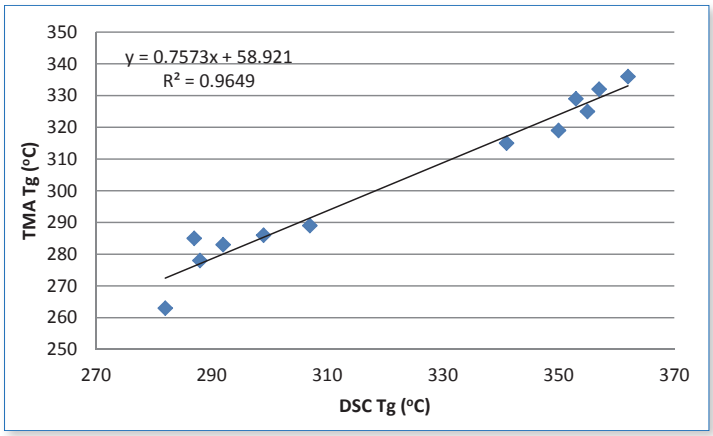

Figure 4—Comparison of the apparent glass transition temperature measured by TMA and DSC.[56]

Differential Scanning Calorimetry

DSC is the most common analytical technique for measuring polymer thermal transitions and is based on the differential in thermal transitions between a sample and a reference material. In particular, DSC measures any thermal transition and is primarily used to quantify the primary and secondary thermal transitions of polymers, liquid coatings, and/or the cure process, and/or finished

Table 2—Techniques and Methodologies for Determining the T_g of Polymeric Materials

Technique	Vertical Abscissa	How T_g is Determined
Differential scanning calorimetry	Heat flow/C_p	Step in C_p/ heat flow
		Peak differential heat flow
Modulated DSC	Heat Flow	Mid-point reversible flow
		Peak differential reversible flow
Dynamic mechanical analysis	Tan δ	Peak tan δ
	Storage modulus	Peak differential storage modulus
Thermomechanical analysis	Deformation	Change in CTE
Dielectric spectroscopy	Dissipation factor	Peak dissipation factor
Fluid confinement dilatometry	Specific volume	Change in V_{sp} slope

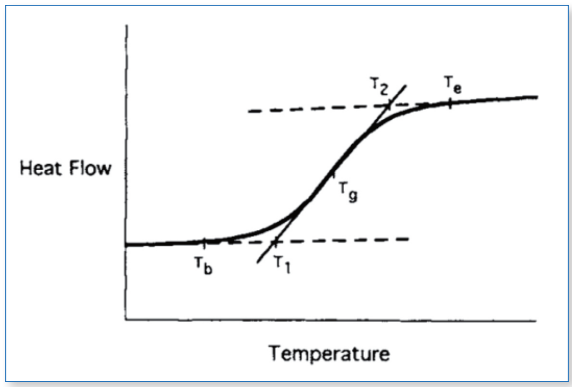

Figure 5—Methods of determining the T_g via DSC: peak derivative (left) and midpoint methods (right). Endotherm up on Y axis.

and cured films.[56,57] Two common methods are used to determine the T_g from a DSC curve: (a) differential curve peak (e.g., evaporation or cure), or (b) the midpoint between extrapolated heat flow rubber and glass baselines, as shown in *Figure* 5 (shifting specific heat values, endotherm is up for *Figure* 5).[56,57] The first time a sample is analyzed, the results are representative of a material's prior historical state and yet, material changes often occur during that evaluation. The first and later thermal analyses often differ for the same sample, whereby most of the thermal history is erased by heating above T_g. Prior environmental exposure can result in thermal behavior shifts as well, e.g., humidity, trapped solvents, physical aging, and annealing.[56,57] The measured T_g is sensitive to differing heating and cooling rates and dramatic differences in T_g values can be observed: the most common heating rate is 10°C/min, while 5 and 20°C /min are also used (but less frequently) in DSC analysis.[56] Slower heating rates provide narrower T_g regions and lower T_g values, but lower signal intensities.

Dynamic Mechanical Analysis

The term DMA covers many forms of mechanical analysis during thermal or frequency-specific characterization. Although distinctly different from calorimetric measurements, the "mechanical" T_g methods of characterization are similar in concept.[56-58] The experimental parameters can be modified to obtain bending, compression, or torsional behavior; environmental chamber attachments are also available, e.g., humidity, immersion. The complex modulus is comprised of the storage modulus (real component) and the loss modulus (imaginary component); the ratio of the loss modulus to the storage modulus is also a well-defined parameter, termed tan δ.[56-58] The T_g in this type of analysis is known as the α transition (mechanical T_g) and can be defined as the tan δ maximum or the storage modulus peak derivative. Subtle or very minute material transitions are often detected and quantified by DMA, e.g., small differences in T_g or modality and ratios of T_g to distinguish between degrees of conversion or multimodal morphological domains — or it can even simultaneously detect cure and solvent evaporation.[56] Since the T_g measured with DMA is both frequency- and ramp rate-dependent, it is very important to note the experimental conditions to objectively discuss and compare the measured T_g.[56]

A REVIEW OF POLYMERS, COATINGS, AND THEIR RELATED T_gS

Modulus Relative to T_g

Polymeric materials are often simplistically described as glassy, leathery, or rubbery. There does not seem to be formal limits for these material types; thus, for general purposes, materials exhibiting room temperature moduli of ≈ 0.5–2 GPa are considered leathery. Rubbery materials range from < 0.001–0.5 GPa, and glassy materials typically possess modulus values between 1.5 – > 100 GPa. *Figure* 6 represents a wide range of material types to illustrate high to low Young's modulus values measured at standard temperature and pressure (STP) conditions.[2,59,60]

As crystallinity influences both the T_g and modulus, it is important to differentiate between amorphous and semicrystalline polymers. The degree of crystallinity may vary substantially between the same composition samples, depending upon formulation variables and thermal history.[2,58] *Figure* 7 lists the T_g of purely amorphous samples of both thermosetting and thermoplastic polymers.

Within a narrow set of building blocks, the typical thermoset polymer will concurrently exhibit high modulus and T_g. Each characteristic is driven by a complex set of parameters; however, in combination, these parameters shift together, e.g., restricted molecular mobility driven by higher density/quantity of crosslinks results in higher T_g. Thermoplastic polymer chains are capable of a wider range of movement in terms of flow or translational motion. Thermoplastic polymers comprised of highly rigid monomers (polyetherimide, for example) exhibit very high T_g and moduli values but are still melt-processable. Rigid backbone structures, bulky side groups that restrict/hinder rotation around the primary chain, and intermolecular interactions all combine to increase T_g and modulus through molecular resistance to motion and flow.[2] Kunal and co-workers found that as the size of a phenyl ring substitution group of polystyrene increased, T_g increased as well, as shown in *Figure* 8, due to congestion of segmental mobility.[63] As these molecular features or barriers to chain rotation and translation are reduced or eliminated, the T_g and modulus decrease. For example, linear

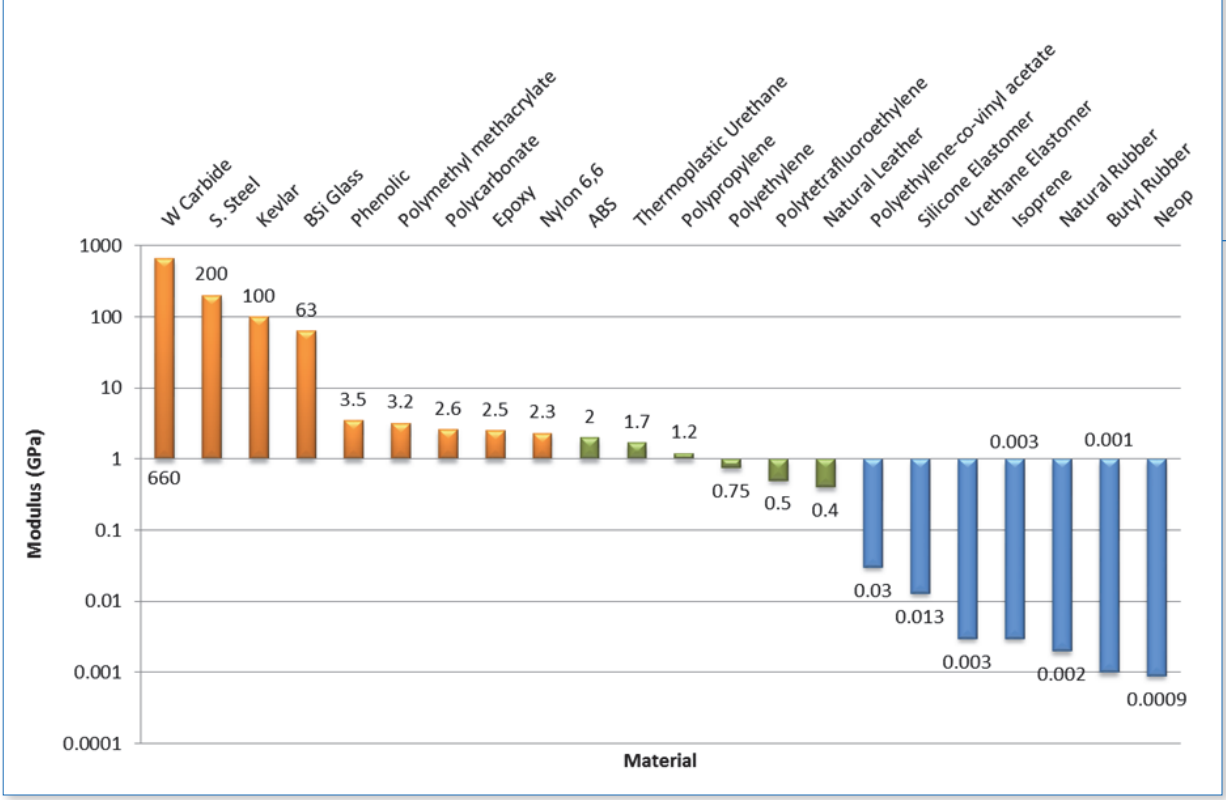

Figure 6—Young's modulus of various polymers and reference materials.[59-62]

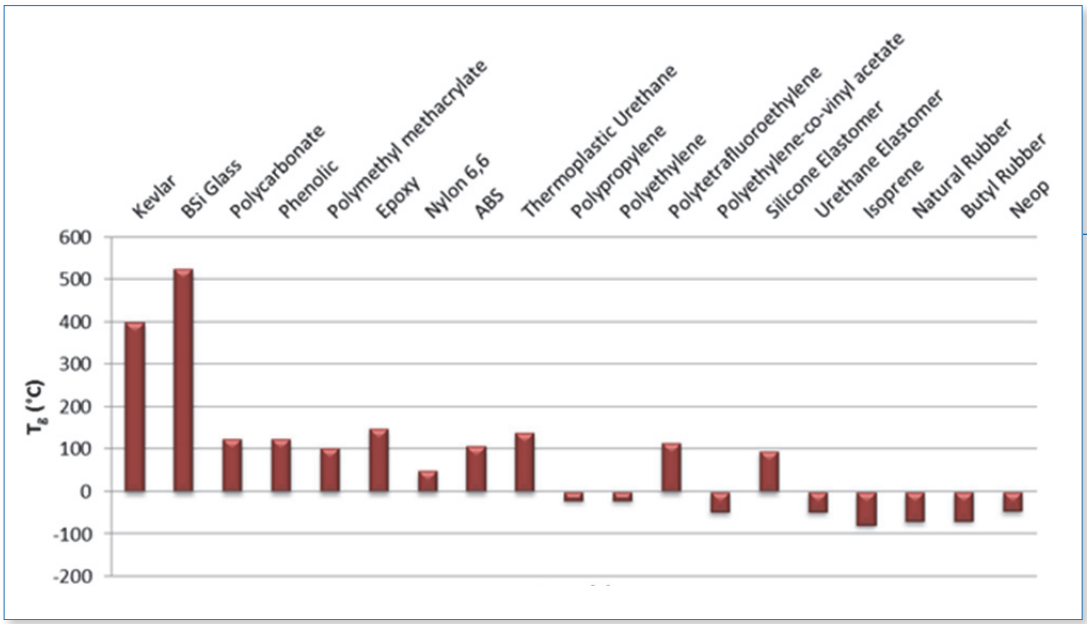

Figure 7—T_g of various polymers and reference materials described in *Figure* 6.[59-62]

aliphatic amorphous polymers are more likely to possess low T_gs (such as high density polyethylene, T_g = 150 K), in contrast to polymers with more rigid backbone structures, e.g., poly(benzimidazole), with a T_g of 773 K.[60-62,64] Lightly crosslinked elastomer rubbers comprised of extremely low T_g building block polymers exhibit low moduli values as chain flexibility increases and allows for less resistance to elastic deformation, as seen in butyl rubber. A correlation exists between Young's modulus and T_g for many amorphous polymeric materials as replotted in *Figures* 9 and 10.

CURE-RELATED T_g CHANGES

In thermosetting systems, the cure and degree of conversion exert substantial influence over T_g development. Multiple models illustrate this concept, e.g., the Hale, Oleinik, and Pascault–Williams models describe the progression of T_g with cure of epoxy-amine systems and have been shown to fit a wide range of thermosetting polymers employed as coatings, composite matrices, and adhesives, among others.[68-72] These models, based primarily upon the empirical DiBenedetto equation as described by Nielsen

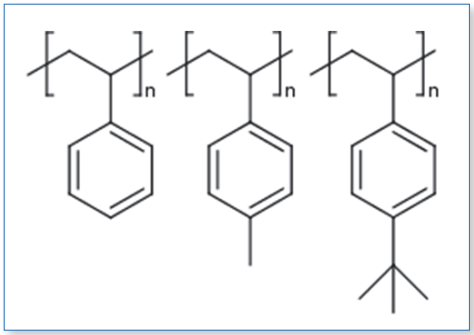

Figure 8—Polystyrene, poly(4-methylstyrene), and poly(t-butylstyrene) were found to exhibit T_gs of ~273, 299, and 318 K, respectively, at n = 8.[63]

have, through experimental support from varying thermoset chemistries, revealed that T_g progression during thermoset cure is dependent upon functionality, conversion, and the extent of crosslinking.[2] Gillham and co-workers investigated the interplay between cure temperature and extent of cure to develop time-temperature-transformation (TTT) diagrams for isothermally cured epoxy-amine systems that can describe many types and classes or conditions for thermosetting polymers (*Figure* 11).[73] As cure temperature increases, T_g also increases due to higher monomer/oligomer molecular weight and ultimately crosslink density

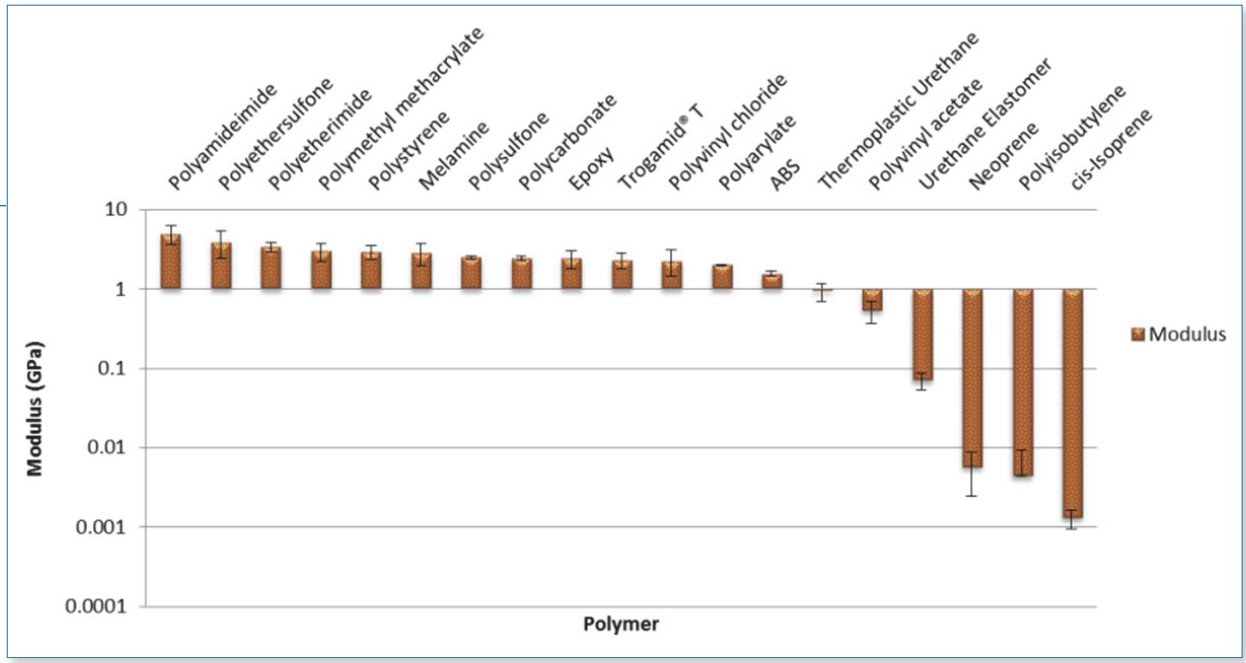

Figure 9—Young's modulus of noncrystalline thermosetting and thermoplastic polymers.[2,61,62,65-67]

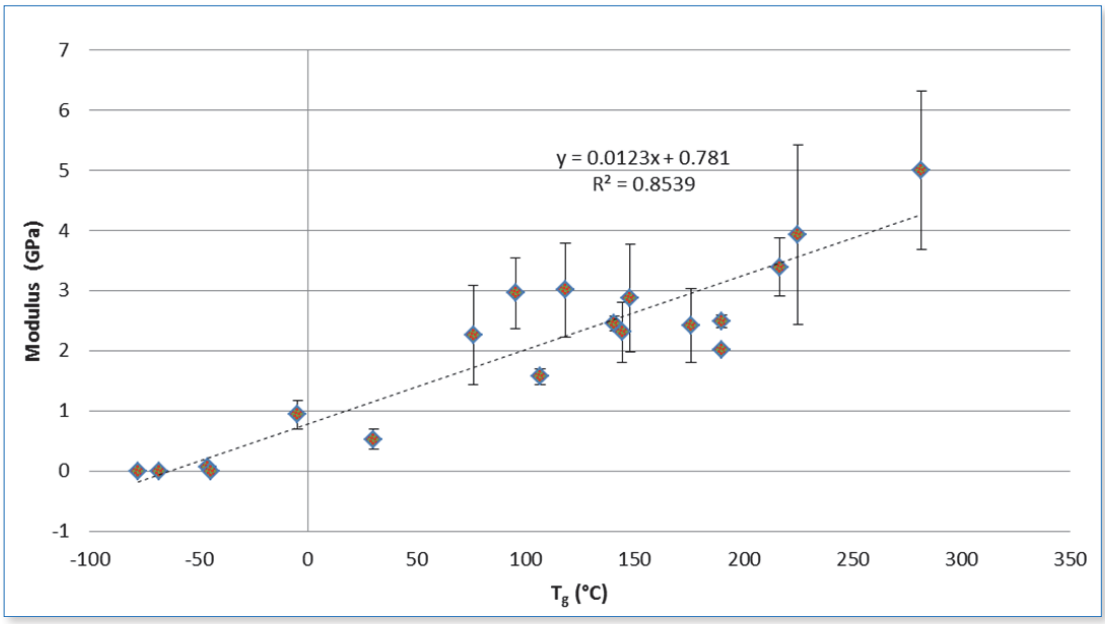

Figure 10—Relationship between Young's modulus and T_g for noncrystalline thermoplastic and thermosetting polymers seen in *Figure* 8. [2,61,62,65-67]

through conversion as well as mobility restrictions driven through additional macromolecular connectivity, while the time to gelation and vitrification decreases. At the same time, the separation between the gelation and vitrification points increases due to decreased mobility concomitant with increased conversion.

Under isothermal cure at various temperatures, the time required to reach the practical infinite glassy T_g diminished, and typically was reached at a higher temperature end point. This was attributed to the mobility available during the early cure process and allowed for the percent reaction of chemical species to reach higher levels.[74,75] The effect of cure-induced changes in these systems was also observed through changes in water diffusion during the course of thermoset cure. As conversion and T_g increased, both the rate of diffusion and equilibrium water uptake increased.[73] These results are often attributed to the development of porosity/free volume as cure proceeds: early in the process, unreacted groups and free oligomers have higher degrees of freedom within the partially developed network volume due to less restricted mobility. As these components are incorporated into the rigid cross-linked network, *trapped* free volume develops which allows for the ingress and permeation of water molecules without the necessity for solvation.[73] Some cure chemistries and mechanisms have been shown to diverge from this trend due to production of condensate, side-reaction, or loss of solvent/plasticizer during cure. Wurster and co-workers investigated the uptake of moisture as a function of cure in the development of polyacrylate-free films and determined that the rate of diffusion decreased while T_g increased during isothermal cure.[76] At extended curing times and higher cure temperatures, an increase in diffusivity was observed that was attributed to thermal oxidative degradation and/or loss of plasticizer, leading to increased porosity.

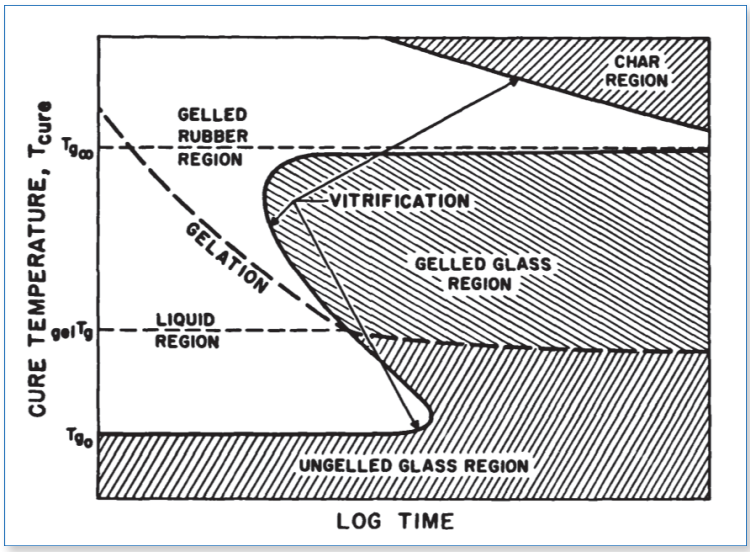

Figure 11—TTT diagram describing the isothermal cure of epoxy-amine thermosetting systems.[68]

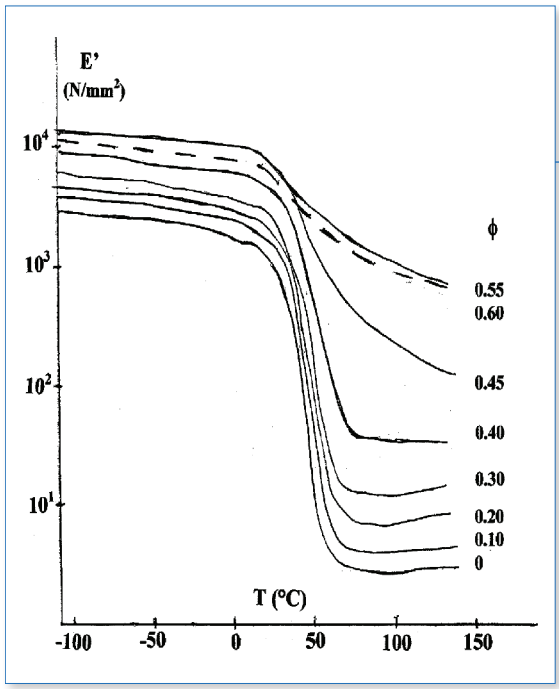

Figure 12—DMA results showing storage modulus on the Y axis and temperature on X axis for a TiO_2 pigmented polyacrylic coating as a function of PVC.[86]

RESULTING FILM FORMATION OF LATEXES

The common and simplistic mechanism for latex film formation is dominated by three main phases: (1) evaporation of primary solvent, resulting in a close-packing formation of the particles, (2) particle deformation and filling in the voids, and (3) polymer self-diffusion across boundaries to yield a continuous film where the original particle shape and locations are no longer distinguishable.[77,78]

There are different mechanisms for the particle deformation phase (phase II) that depend upon several processing variables such as: (1) wet sintering, when particle deformation times are shorter than solvent evaporation times with respect to vertical water level, (2) dry sintering, when deformation primarily occurs in the absence of water, (3) capillary deformation, when capillary forces during water evaporation exceed the stress requirement for particle deformation, and (4) the receding water front mechanism, a combination of capillary deformation and dry sintering. Routh and Russel developed a model to predict which mechanism will operate under a given set of conditions. Gonzalez and co-workers employed this model

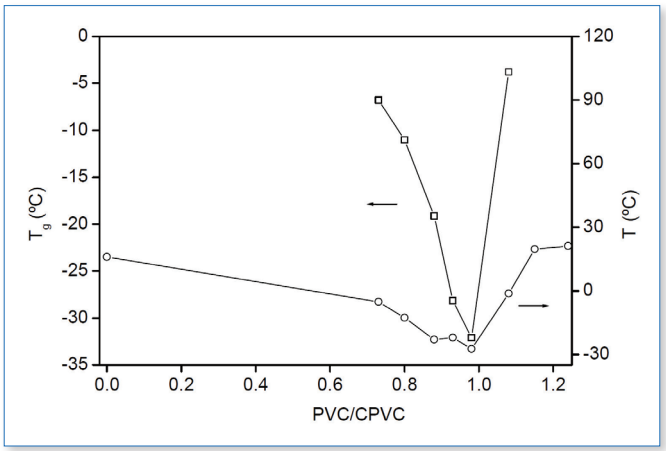

Figure 13—Thermal relaxation differences comparing T_g (DSC) and T_α (DMA tan δ mechanical relaxation) values of a pigmented epoxy-amine coating as a function of reduced PVC.[87]

in the form of a Routh–Russel deformation map to achieve low defect films from latexes with T_g of 45, 55, and 64°C without any coalescence aids that constitute VOCs.[77,79-81]

EFFECT OF HYDROPLASTICIZATION ON LATEX FILM FORMATION

The effect of water and humidity on latex film formation depends greatly on the polymer particle. An important property to consider for latex film formation is the self-diffusion coefficient. Feng and Winnik showed that for the relatively hydrophobic polymer PBMA, water had little effect on diffusion, but for the copolymer, P(MAA-co-BMA), water aided diffusion.[82] The more hydrophilic polymer also contained higher residual water content. Interestingly, PBMA films exposed to 100% RH or immersed in water for sufficient time resulted in reversible film turbidity, while the more hydrophilic copolymer P(MAA-co-BMA) remained transparent.[82] Sperry and co-workers observed that minimum film formation temperatures (MFFT) were time-dependent, different humidity levels and processing parameters altered the MFFT, and humidity has a greater effect on more hydrophobic polymer particles.[83] Using fluorescence resonance energy transfer (FRET) spectroscopy to study film formation under different conditions, Haley and co-workers concluded that high humidity retards coalescence of P(BA-co-MMA) as the residual water between particles acts as a barrier.[84] Although this slows the beginning of polymer diffusion, the higher humidity eventually increases hydroplasticization effects, resulting in increased diffusion rates once diffusion is allowed.[84] It is suggested that the greater affinity of more hydrophilic polymers for water allows the formation of "water films" that retard polymer self-diffusion.[84] An interesting study of the effects of humidity on polymer self-diffusion using polymers designed to have equivalent T_g with different hydrophilicities, by Soleimani and co-workers, showed that water uptake and effective shift factors, paralleling WLF temperature shift factors, do not follow a linear relationship with water uptake.[85] They proposed that only water that was molecularly dispersed had sufficient hydroplasticizing effects on polymer self-diffusion, and that pockets of water eventually develop during film formation and phase separation giving the observed turbid films.[85]

PIGMENTATION EFFECTS ON T_g AND MODULUS

Figures 12 and 13 describe the influence of pigmentation on the T_g as measured using DMA (*Figure* 12) and both DSC and DMA over a range of pigment volume concentration (PVC) (*Figure* 13, plotted as volume fraction of pigment). CT

****

Part II of this article will be published in the September 2014 issue of CoatingsTech.

References

1. Schmelzer, J.W.P. and Gutzow, I.S., *Glasses and the Glass Transition*, Wiley-VCH: Weinheim, Germany, 2011.
2. van Krevelen, D.W. and Nijenhuis, K. te., *Properties of Polymers*, 4th Ed., Elsevier: Oxford, UK, 2009.
3. Taylor, J.W. and Klots, T.D., *Proc. Waterborne, Higher Solids and Powder Coatings Symp.,* 181, 2002.
4. Tsavalas, J.G. and Sundberg, D.C., *Langmuir*, *26*, 6960 (2010).
5. Lesikar, A.V., *J. Chem. Phys.*, *63*, 2297 (1975).
6. Sare, E.J. and Angell, C.A., *J. Solution Chem., 2*, 53 (1973).
7. Wang, L.-M. and Richert, R., *J. Chem. Physics, 120*, 11082 (2004).
8. Lesikar, A.V., *J. Phys. Chem., 80*, 1005 (1976).
9. Greenspan, H. and Fischer, E., *J. Phys. Chem., 69*, 2466 (1965).
10. Mirkhani, S.A., Gharagheizi, F., Ilani-Kashkouli, P., and Farahani, N., *Thermochim Acta, 543*, 88 (2012).
11. Dawson, K.A., *Current Opinion in Colloid & Interface Science*, *7*, 218 (2002).
12. Matveev, Y.I., Grinberg, V.Y., Sochava, I.V., and Tolstoguzov, V.B., *Food Hydrocolloid, 11*, 125 (1997).
13. Ringe, D. and Petsko, G.A., *Biophys. Chem.*, *105*, 667 (2003).
14. Tsai, A.M., Udovic, T.J., and Neumann, D.A., *Biophys. J.*, *81*, 2339 (2001).
15. Ngai, K.L., Capaccioli, S., Shinyashiki, N., *J. Phys. Chem. B*, *112*, 3826 (2008).
16. Jansson, H. and Swenson, J., *Bba-Proteins Proteom*, *1804*, 20 (2010).
17. Doster, W., *Biochimica et Biophysica Acta (BBA) - Proteins and Proteomics*, *1804*, 3 (2010).

18. Cummins, H.Z., Zhang, H., Oh, J., Seo, J.-A., Kim, H.K., Hwang, Y.-H., Yang, Y.S., Yu, Y.S., and Inn, Y., *J. Non-Cryst. Solids*, *352*, 4464 (2006).
19. Simperler, A., Kornherr, A., Chopra, R., Jones, W., Motherwell, W.D., and Zifferer, G., *Carbohydrate Res.*, *342*, 1470 (2007).
20. Roe, K.D. and Labuza, T.P., *Int. J. Food Prop.*, *8*, 559 (2005).
21. De Gusseme, A., Carpentier, L., Willart, J.F., and Descamps, M., *J. Phys. Chem., B*, *107*, 10879 (2003).
22. Avramov, I., Vassilev, T., and Penkov, I., *J. Non-Cryst. Solids*, *351*, 472 (2005).
23. Steinberg, J. and Lord, A.E., *J. Am. Ceram. Soc.*, *63*, 234 (1980).
24. Deubener, J., Muller, R., Behrens, H., and Heide, G., *J. Non-Cryst. Solids*, *330*, 268 (2003).
25. Naftaly, M. and Miles, R.E., *J. Appl. Phys.*, *102* (2007).
26. Sulowska, J., Wacawska, I., and Szumera, M., *J. Therm. Anal. Calorim.*, *109*, 705 (2012).
27. Sayer, M. and Mansingh, A., *Phys. Rev. B*, *6* (1972).
28. Brow, R.K., *J. Non-Cryst. Solids*, *263–264*, 1 (2000).
29. Hoppe, U., *J. Non-Cryst. Solids*, *195*, 138 (1996).
30. Shih, P.Y., *Mater. Chem. and Phys.*, *84*, 151 (2004).
31. Vitale-Brovarone, C., Novajra, G., Milanese, D., Lousteau, J., and Knowles, J.C., *Mater. Sci. Eng. C-Mater.*, *31*, 434 (2011).
32. Sobha, K.C. and Rao, K.J., *J. Non-Cryst. Solids*, *201*, 52 (1996).
33. Mitachi, S., Terunuma, Y., Ohishi, Y., Takahashi, S., *J. Lightwave Technol.*, *2*, 587 (1984).
34. Tran, D., Sigel, G., and Bendow, B., *J. Lightwave Technol.*, *2*, 566 (1984).
35. Rault, G., Adam, J.L., Smektala, F., Lucas, J., *J. Fluorine Chem.*, *110*, 165 (2001).
36. Trnovcova, V., Zakalyukin, R.M., Sorokin, N.I., Lezal, D., Fedorov, P.P., Illekova, E., Ozvoldova, M., Skubla, A., and Sobolev, B.P., *Ionics*, *7*, 456 (2001).
37. Sanditov, B.D., Sangadiev, S.S., and Sanditov, D.S., *Polym. Sci. Ser. A*, *48*, 1263 (2006).
38. Lu, Z.P. and Liu, C.T., *Acta Mater.*, *50*, 3501 (2002).
39. Sperling, L.H., *Introduction to Physical Polymer Science*, John Wiley & Sons, Inc.: Hoboken, New Jersey, 2005.
40. Ojovan, M., *Entropy*, *10*, 334 (2008)
41. Young, R.J. and Lovell, P.A. (Eds.), *Introduction to Polymers, Third Edition*, CRC Press, 2011.
42. Massa, D.J. and Flick, J.R., *Polym. Prepr., Am. Chem. Soc., Div. Polym. Chem.*, *14*, 1249 (1973).
43. Bai, Y. and Keller, T., *High Temperature Performance of Polymer Composites*, John Wiley & Sons: Weinheim, Germany, 2013.
44. Zeleznak, K. and Hoseney, R., *Cereal Chem.*, *64*, 121 (1987).
45. Simha, R. and Boyer, R.F., *J. Phys. Chem.*, *37*, 1003 (1962).
46. Budd, P.M., McKeown, N.B., and Fritsch, D., *J. Mater. Chem.*, *15*, 1977 (2005).
47. Daniels, C.A., *Polymers: Structure and Properties*, Technomic Publishing Company: Lancaster, PA, Vol. 22, 1989.
48. Kovacs, A., *Fortschritte der Hochpolymeren-Forschung*, *3*, 394 (1964).
49. McKenna, G.B., In *Comprehensive Polymer Science*, Booth, C., Price, C. (Eds.), Pergamon: Oxford, Vol. 2, "Polymer Properties," p 311, 1989.
50. Vogel, H., *Physikalische Zeitschrift*, *22*, 645 (1921).
51. Fulcher, G.S., *J. Am. Ceramic Soc.*, *8*, 339 (1925).
52. Tammann, G. and Hesse, W., *Zeitschrift für anorganische und allgemeine Chemie*, *156*, 245 (1926).
53. Williams, M.L., Landel, R.F., and Ferry, J.D., *J. Am. Chem. Soc.*, *77*, 3701 (1955).
54. Kovacs, A. J., *J. Polym. Sci.*, *30*, 131 (1958).
55. Scherer, G., *Relaxation in Glass and Composites*, Wiley: New York, 1986.
56. van Ekeren, P.J., *Handbook of Thermal Analysis and Calorimetry: Applications to Polymers and Plastics*, Vol. 3, Elsevier Science B.V.: Amsterdam, 2003.
57. Naranjo, A., Noriega, M.d.P., Osswald, T., Alejandro, R.-A., and Sierra, J.D., *Plastics Testing and Characterization: Industrial Applications*, Hanser Gardner Publishers: Cincinnati, 2008.
58. Hiemenz, P.C. and Lodge, T.P., *Polymer Chemistry*, 2nd Ed., CRC Press: Boca Raton, FL, 2007.
59. Ashby, M.F., *ATB Metall.*, *33*, 33 (1993).
60. Ashby, M.F. and Jones, D.R.H., *Engineering Materials Two. Introduction to Microstructures, Processing, and Design*, Pergamon: Amsterdam, 1986.
61. Corneliussen, R.D., *Modern Plastics Encyclopedia 1999*, McGraw-Hill: New York, 2002.
62. Matsuoka, S., In *Handbook of Thermal Analysis and Chemistry*, Elsevier Science B.V., Vol. 3, p 125 (2002).
63. Kunal, K., Robertson, C.G., Pawlus, S., Hahn, S.F., and Sokolov, A.P., *Macromolecules (Washington, DC, U.S.)*, *41*, 7232 (2008).
64. Anon., *J. Am. Chem. Soc.*, *131*, 16330 (2009).
65. Chanda, M. and Roy, S.K., *Plastics Technology Handbook*, 3rd ed., Taylor and Francis: Boca Raton, FL, 1998.
66. Kauffman, G.B., *J. Chem. Educ.*, *87*, 479 (2010).
67. CAMPUSPlastics Online Database, Styrolution Terlux MABS, http://www.campusplastics.com/campus/brandproducer/Styrolution+Group+GmbH/654, accessed 2013.
68. Urbaniak, M., *Polimery* (Warsaw, Pol.), *56*, 240 (2011).
69. Guenthner, A.J., Reams, J.T., Lamison, K.R., Cambrea, L.R., Vij, V., and Mabry, J.M. *Int. SAMPE Tech. Conf.*, *43* (2011).
70. Hadiprajitno, S., Hernandez, J.P., and Osswald, T.A., *61st Annual Tech. Conf., Soc. Plast. Eng.*, 818 (2003).
71. Li, Y. and Morgan, R.J., *Proc. 33rd NATAS Annu. Conf. Therm. Anal. Appl.*, 009.48.305/1 (2005).
72. Sabzevari, S.M., Alavi-Soltani, S., Koushyar, H., and Minaie, B., *SAMPE Conf. Proc.*, *55*, sabze4/1 (2010).
73. Enns, J.B. and Gillham, J.K., *J. Appl. Polym. Sci.*, *28*, 2831 (1983).
74. Wisanrakkit, G. and Gillham, J.K., *Adv. Chem. Ser.*, *227*, 143 (1990).
75. Zarrelli, M., Skordos, A.A., and Partridge, I.K., *Plast., Rubber Compos.*, *31*, 377 (2002).
76. Wurster, D.E., Bhattacharjya, S., and Flanagan, D.R., *Aaps Pharmscitech*, *8*, E71 (2007).
77. Routh, A.F. and Russel, W.B., *Langmuir*, *15*, 7762 (1999).
78. Chen, X., Fischer, S., and Men, Y., *Langmuir: J. Surf. and Colloids*, *27*, 12807 (2011).
79. Gonzalez, E., Paulis, M., Barandiaran, M.J., and Keddie, J.L., *Langmuir: J. Surf. and Colloids, 29*, 2044 (2013).
80. Routh, A.F. and Russel, W.B., *Ind. & Engin. Chem. Res., 40*, 4302 (2001).

81. Routh, A.F. and Russel, W.B., *Langmuir*, *17*, 7446 (2001).
82. Feng, J. and Winnik, M.A., *Macromolecules*, *30*, 4324 (1997).
83. Sperry, P.R., Snyder, B.S., O'Dowd, M.L., and Lesko, P.M., *Langmuir*, *10*, 2619 (1994).
84. Haley, J.C., Liu, Y., Winnik, M.A., and Lau, W., *J. Coat. Technol. Res.*, *5*, 157 (2008).
85. Soleimani, M., Haley, J.C., Lau, W., and Winnik, M.A., *Macromolecules*, *43*, 975 (2010).
86. Mills, N., *Plastics: Microstructure and Engineering Applications*, 3rd Ed., Butterworth-Heinemann: Burlington, 2005.

AUTHORS

Greg Curtzwiler, **Mark Early**, **Diana Gottschalk**, **Christina Konecki, Robert Peterson**, **Steven Wand** and **James W. Rawlins**,
School of Polymers and High Performance Materials,
The University of Southern Mississippi,
118 College Drive #5217, Hattiesburg, MS 39406;
james.rawlins@usm.edu.